# Characterization of an Autoreduction Pathway for the $[Fe_4S_4]^{3+}$ Cluster of Mutant *Chromatium vinosum* High-Potential Iron Proteins. Site-Directed Mutagenesis Studies To Probe the Role of Phenylalanine 66 in Defining the Stability of the $[Fe_4S_4]$ Center Provide Evidence for Oxidative Degradation via a $[Fe_3S_4]$ Cluster[†]

Shumin Bian, C. F. Hemann, Russ Hille, and J. A. Cowan*

*Evans Laboratory of Chemistry, The Ohio State University, 100 West 18th Avenue, Columbus, Ohio 43210*

*Received July 9, 1996*[⊗]

ABSTRACT: A number of point mutations of the conserved aromatic residue phenylalanine 66 (Phe66Tyr, -Asn, -Cys, -Ser) in *Chromatium vinosum* high-potential iron sulfur protein have been examined with the aim of understanding the functional role of this residue. Nonconservative replacements with polar residues have a minimal effect on the midpoint potential of the $[Fe_4S_4]^{3+/2+}$ cluster, typically $<+25$ mV, with a maximum change of $+40$ mV for Phe66Asn. With the exception of the Phe66Tyr mutant, the oxidized state was found to be unstable relative to the recombinant native, with regeneration of the reduced state. The pathway for this transformation involves degradation of the cluster in a fraction of the sample, which provides the reducing equivalents required to bring about reduction of the remainder of the sample. This degradative reaction proceeds through a transient $[Fe_3S_4]^{+}$ intermediate that is characterized by typical *g* values and power saturation behavior and is prompted by the increased solvent accessibility of the cluster core in the nonconservative Phe66 mutants as evidenced by $^{1}H-^{15}N$ HMQC NMR experiments. These results are consistent with a model where the critical role of the aromatic residues in the high-potential iron proteins is to protect the cluster from hydrolytic degradation in the oxidized state.

High-potential iron proteins (HiPIP's)[1] are a structurally well-defined class of iron−sulfur cluster protein that afford a useful paradigm for structure−function studies of the role of the protein matrix in defining the chemistry and functional properties of the $[Fe_4S_4]^{3+/2+}$ prosthetic unit (Carter et al., 1974a; Carter, 1977; Rayment et al., 1992), including the stability, redox chemistry, and metal lability of the 4Fe center. A clear understanding of the molecular mechanisms underlying the chemistry of metalloredox cofactors promises to afford the insight required to engineer catalytic and redox centers of technological value and provides insight on biologically relevant cluster assembly/disassembly pathways (Pagani et al., 1984; Flint, 1996; Flint et al., 1993, 1996). To this end we have cloned and overexpressed a synthetic gene encoding the sequence for the high-potential iron protein from the photosynthetic bacterium *Chromatium vinosum* (Agarwal et al., 1993). This expression system has already been used to advantage in studies of the functional role of the conserved hydrophobic aromatic residues that form a binding pocket for the $[Fe_4S_4]$ cluster (Lui & Cowan, 1994; Agarwal et al., 1995; Li et al., 1996a,b). Several proposals have been made for the importance of such residues, which include fine tuning of the unusually high reduction potential of HIPIP as a result of favorable bonding interactions with the cluster, maintenance of a low dielectric solvent-free environment, or involvement in electron exchange pathways (Carter et al., 1974b; Bertini et al., 1993; Mizrahi et al., 1980; Jensen et al., 1994). Residue Phe66 is of particular interest since it lies in close proximity to the cluster and is a nonconserved residue relative to the HiPIP from the bacterium *Rhodocyclus tenuis* (Rayment et al., 1992), which shows an isoleucine residue at that site. For this protein the midpoint potential is 50 mV lower than that of *C. vinosum* HIPIP (Przysieck et al., 1985).

In this paper we characterize several conservative and nonconservative Phe66 mutants of *C. vinosum* HiPIP. In spite of some perturbations of signals in the NMR and EPR spectra, the reduction potentials of these mutants display only minor perturbations relative to recombinant native. More importantly, we demonstrate a requirement for the aromatic ring to maintain the stability of the iron−sulfur cluster in the oxidized state. The oxidative instability observed for many of the mutant proteins is a consequence of the increased solvent accessibility of the cluster core. In the course of these studies, a novel HiPIP degradation intermediate has been identified and characterized as a $Fe_3S_4$ cluster. While many examples of the formation of $[Fe_3S_4]$ centers have been reported for low-potential ferredoxin-like centers, arising from ferricyanide or air oxidation of the cluster (Thomson et al., 1981; Johnson et al., 1982; Bell et al., 1982; Moura et al., 1982), or from Cys mutations (Rothery & Weiner, 1991; Kowal et al., 1995), this is only the second reported example of the transient formation of a 3Fe cluster in a high-potential iron−sulfur protein and differs from the degradative intermediate previously reported from our laboratory for the Cys77Ser mutant (Agarwal et al., 1996) which involved a directly coordinating residue.

[†] This work was supported principally by the National Science Foundation from Grants CHE-8921468 (J.A.C.) and MCB-9420185 (R.H.). J.A.C. is a Camille Dreyfus Teacher−Scholar (1994−1999) and a National Science Foundation Young Investigator (1992−1997).

[⊗] Abstract published in *Advance ACS Abstracts,* November 1, 1996.

[1] Abbreviations: HiPIP, high-potential iron protein; NMR, nuclear magnetic resonance; COSY, 2D correlation spectroscopy; HMQC, heteronuclear multiple quantum correlated spectroscopy.

S0006-2960(96)01658-3 CCC: $12.00 

## EXPERIMENTAL METHODS

*Enzymes, Chemicals, and Bacterial Strains.* Restriction and modifying enzymes were purchased from BRL (Life Technologies, MD), and DTT and IPTG were obtained from Boehringer Mannheim (Indianapolis, IN). *Escherichia coli* strain XL-1 blue was used for routine site-directed mutagenesis and plasmid storage, strain RZ1032 was used for preparation of single-strand DNA for mutagenesis, and strain BL21 (DE3) plys S served as a host for protein expression. Helper phage VCS M13 for rapid single-strand rescue of DNA from the pET21d(+) phagemid was obtained from Stratagene (La Jolla, CA). General molecular biology procedures were followed from Sambrook et al. (1989).

*Plasmid Construction, Site Directed Mutagenesis, and Nucleotide Sequencing.* Construction of the plasmid pET21d-(+)-HIPIP, encoding the entire gene region for *C. vinosum* HIPIP, has been described elsewhere (Agarwal et al., 1993). Mutagenesis was performed according to the method of Kunkel et al. (1987). The oligonucleotide primer for mutagenesis was 27-mer in length and was designed with redundancies at the mutation site to allow isolation of discrete plasmids bearing point mutations. Specifically, TTC (Phe) was engineered to TAC (Tyr), AGC (Ser), TGC (Cys), AAC-(Asn), CGC (Arg), and CAC(His); however, only plasmids bearing the first four mutations listed were identified during exhaustive screening. Uracil-enriched template pET21d(+)-HIPIP was obtained from the $dut^-$ $ung^-$ *E. coli* strain RZ1032 and grown in 2 × TY medium with the helper phage VCSM13. All mutations were finally characterized and confirmed by DNA sequencing according to the Sequenase protocol (United States Biochemical Corp., Cleveland, OH).

*Protein Isolation.* Cultures were grown, expression was induced by IPTG, and protein was purified as previously described for recombinant native (Agarwal et al., 1993). When necessary, further purification was carried out by FPLC on a Mono Q column (1 × 5 cm) using nondenaturing conditions. Optimal separation of bands was obtained by a gradient method, using two stocks of degassed phosphate buffer, at pH 7.5 (A, 10 mM phosphate; B, 10 mM phosphate, 500 mM NaCl). The total running time was 20 min (3 min with 0% B and 17 min from 0 to 100% B).

*Autoreduction of Oxidized Mutants.* Kinetic data were obtained at an ambient temperature of 295 K by monitoring the decrease in absorbance at 500 nm for oxidized mutant proteins by use of a Hewlett-Packard 8452A diode array spectrophotometer. Typical experimental conditions included a solution of 20 $\mu$M HiPIP in 10 mM sodium phosphate buffer with 0.1 M NaCl (pH 6.0). The protein concentration was determined by use of the extinction coefficients for the reduced native protein, $\epsilon_{282} \sim 41.3$ $mM^{-1}$ $cm^{-1}$ and $\epsilon_{388} \sim 16.1$ $mM^{-1}$ $cm^{-1}$. This is justified by the observation that the $A_{282}/A_{388}$ ratio was similar for the native and mutant HiPIP's (Table 1). Approximately 100 $\mu$M oxidant was added from a concentrated stock solution and the assay started immediately after mixing by inversion. The trace of an assay (OD decay at 500 nm) was then fitted to a single-exponential curve and the first-order rate constant obtained from the fitting. Rate constants are summarized in Table 2.

*NMR Spectroscopy.* 1D and 2D COSY NMR spectra of Phe66 mutants were acquired as previously described (Agarwal et al., 1995; Li et al., 1996). 1D spectra were acquired using a SUWEFT pulse sequence to optimize signal intensities and resolution of the paramagnetically shifted resonances (Inubushi & Becker, 1983), while effective solvent suppression was maintained. Samples dissolved in $H_2O$ contained 10% (v/v) $D_2O$ for the lock. 2D COSY experiments were acquired using the standard pulse program COSYPR with solvent suppression.

For the $^1H/^2H$ exchange experiments (Li et al., 1996b), the $^{15}N$-labeled native and mutant HiPIP samples were lyophilized and then redissolved in $D_2O$ immediately before NMR data acquisition. The $^1H/^2H$ exchange experiments were performed on a Bruker DMX 600 instrument using a standard $^1H-^{15}N$ HMQC pulse sequence (Palmer et al., 1991; Kay et al., 1992; Schleucher et al., 1993). Each 2D HMQC data set was collected in a time frame of less than 12 min for a spectrum defined by a 2K ($t_2$) × 256 ($t_1$) data matrix, with four scans for each $t_1$ increment and an initial 16 dummy scans sufficing for the entire experiment. As a result of the large memory and digital filter capabilities of the DMX instrument, the time typically spent on collecting dummy scans before $t_1$ data collection and on saving each $t_1$ data set was eliminated. The delay time that distinguished each experiment was calculated from the time when the lyophilized sample was dissolved in $D_2O$ to the midpoint of each experiment. Cross-peak intensities were found to diminish with increasing delay time.

*EPR.* EPR spectra were recorded at X-band with a Bruker ESP 300 spectrometer equipped with an Oxford liquid helium cryostat and an internal integration program in the Bruker software package. The temperature was measured by use of a Au/Fe vs Cr thermocouple. Experimental parameters are listed in footnotes to the tables and figure legends. Spin quantitations were carried out under nonsaturating conditions using native oxidized HiPIP as a reference. Data for both samples and standard were obtained using the same buffer conditions. Spectra were obtained of an anaerobic solution of 0.7 mM protein in 10 mM sodium phosphate buffer (pH 7.0) at a variety of temperatures and power levels.

EPR spin quantitation of intermediates produced during decomposition of the oxidized mutant HiPIP's (such as that shown in Figure 6) was performed using the Aasa−Vanngard equation (Aasa & Vanngard, 1975; Fee et al., 1975), relative to the standard oxidized form, and half-power saturation levels ($P_{1/2}$) were estimated by use of the standard empirical equation

$$S = K[P/(1 + P/P_{1/2})^b]^{1/2}$$

where $S$ is the signal amplitude, $P$ is the applied power, $K$ is a proportionality factor, and $b$ is the inhomogeneity parameter (Innes & Brudvig, 1989). The latter typically has a value between 1 and 3 and can be approximated as 1 in the limit of inhomogeneously broadened lines.

## RESULTS

*Expression and Characterization of Mutants.* A 27-mer oligonucleotide mutagenic primer, 5′-CAGTTTACCCGGG-(TC)(AGT)AAGTTGGCAACC-3′, was designed with redundancies to provide a range of aromatic, hydrophobic, hydrophilic, and charged side-chain residues. Four mutants (Phe66Ser, Cys, Tyr, Asn) were identified and expressed in *E. coli* as holoproteins and isolated in the reduced form

Table 1: Ratios of Extinction Coefficients for Reduced Rec-native and Mutant HiPIP's

| | rec-native | Phe66Tyr | Phe66Cys | Phe66Ser | Phe66Asn |
|---|---|---|---|---|---|
| $A_{282}$ nm/ $A_{388}$ nm[a] | 2.36 | 2.88 | 2.69 | 2.76 | 2.71 |

[a] For the reduced rec-native protein, $\epsilon_{282} \sim 41.3$ mM$^{-1}$ cm$^{-1}$ and $\epsilon_{388} \sim 16.1$ mM$^{-1}$ cm$^{-1}$ (Bartsch, 1978).

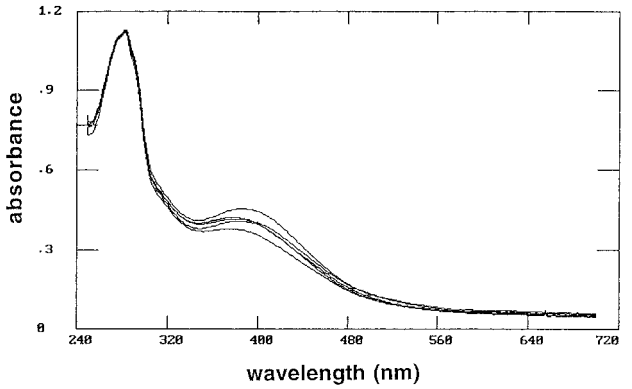


FIGURE 1: Optical spectra of native and mutant derivatives of reduced *C. vinosum* HiPIP. Spectra were taken in 10 mM potassium phosphate buffer containing 100 mM NaCl (pH 7). The spectra in order of decreasing intensity at 388 nm correspond to rec-native, Phe66Cys, Phe66Asn, Phe66Tyr, and Phe66Ser.

following standard protocols (Agarwal et al., 1993). Expression yields for mutants (~10 mg/L) were considerably lower than for recombinant native protein (~30 mg/L). In the reduced state, the mutants were stable and could be maintained as frozen stocks (−20 °C) for many weeks. In the oxidized state, the mutant proteins were generally unstable over a time frame of 1−2 h, following a stability order Phe66Tyr ≫ Ser > Cys > Asn. The origins of this instability are described later.

A detailed electrochemical characterization of these, and other mutants, has been described elsewhere (Soriano et al., 1996), including an evaluation of enthalpic and entropic components and electron self-exchange rates. The potentials for each of the mutants were found to be higher than that of the native. Mutant Phe66Tyr has a potential very close to native, while Phe66Ser and Phe66Cys are moderately (~15 mV) higher. The most significant change was found for the Phe66Asn mutant with an increase of ~40 mV relative to the native protein.

The optical spectra for reduced native and mutant proteins are similar, with two absorbance bands at 282 and 388 nm (Table 1 and Figure 1). Following addition of a 5-fold excess of potassium ferricyanide, the mutant proteins formed brown solutions characteristic of the oxidized form (Bartsch, 1978). After rapid removal of excess oxidant by passage through a short G-25 column (0.8 cm × 2.5 cm), the optical spectra were generally found to be similar to oxidized native with a shoulder on the principal cluster absorbance at around 420−450 nm; however, with the exception of the Phe66Tyr derivative, the spectra for the oxidized mutants were observed to revert to the reduced form over a period of 20 min to 2 h (Figure 2) and formation of some reduced Phe66Asn mutant was usually observed immediately following gel filtration chromatography. The Phe66Tyr mutant slowly returns to the reduced state in a single-exponential process with a first-order rate constant of 0.002 min$^{-1}$. The Phe66Cys and

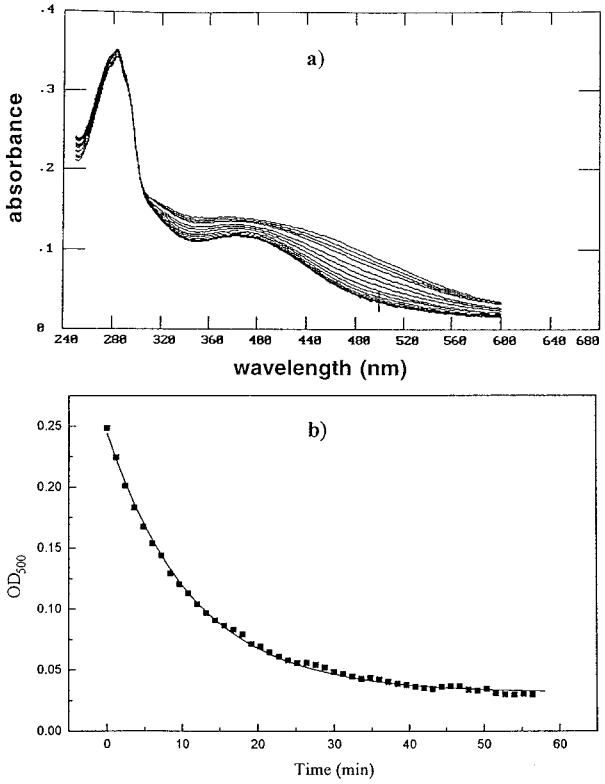


FIGURE 2: Kinetic decay trace of oxidized mutant HiPIP (Phe66Ser) in the presence of a 10-fold excess of $K_3IrCl_6$ oxidant. The protein was dissolved in 10 mM potassium phosphate buffer containing 100 mM NaCl, pH 7. (a) Optical spectral changes as a function of time from the oxidation event showing the change from oxidized (top) to reduced (bottom) protein. (b) Change in the optical density at 500 nm as a function of time.

Phe66Ser mutants were observed to undergo autoreduction more rapidly with first-order rate constants of 0.03 and 0.09 min$^{-1}$, respectively. The Phe66Asn mutant demonstrated the most rapid autoreduction rate of ~0.17 min$^{-1}$.

A number of control experiments were carried out to characterize the origin of the autoreduction phenomenon. The influence of oxidant potential was examined by comparing the effect of two species, $[Fe(CN)_6]^{3-/4-}$ ($E_m \sim 420$ mV) and $[IrCl_6]^{-/2-}$ ($E_m \sim 890$ mV), on the stability of oxidized HiPIP Phe66Ser, Phe66Cys, and Phe66Asn mutants. Autoreduction was observed with either oxidant, even in the presence of up to 20-fold excess of reagent.

Given the tendency of the protein to undergo reduction, even in the presence of excess oxidant, we considered the possibility that the reducing equivalent might originate from an internal source. As described later, the reduction potentials for the mutant proteins are close to that of native, and so the absence of such an internal oxidation for the native protein would have to be ascribed to kinetic factors. We regarded it as unlikely that the electron donor would be the residue at position 66, since one might expect the Phe66Cys mutant to show the faster autoreduction rate as a result of the more effective thiol reductant.

A third possibility, and one that appears consistent with the available data, follows from the apparent hydrolytic instability of the oxidized cluster in most of the mutant HiPIP's. The release of ferrous ion and sulfide provides reducing equivalents for the remaining oxidized protein, giving rise to an apparent autoreduction pathway. The evidence for this proposal will be presented later in the paper.

Table 2: Autoreduction Rate Constants for Oxidized HiPIP at 295 K

| | rate constants ($min^{-1}$) | | | |
|---|---|---|---|---|
| | Phe66Tyr | Phe66Cys | Phe66Ser | Phe66Asn |
| ferricyanide present | 0.002 | 0.02 | 0.09 | 0.17 |
| ferricyanide absent[a] | 0.002 | 0.03 | 0.09 | ~0.2[b] |
| hexachloroiridate present | 0.002 | 0.05 | 0.06 | 0.08 |

[a] Excess ferricyanide was removed immediately after oxidation by passage through a G-25 column. [b] This value is estimated since the mutant becomes partially reduced during chromatographic removal of excess oxidant.

Table 2 shows that for either oxidant the autoreduction of the mutant proteins follows the same trend, with Phe66Asn being the most unstable and Phe66Tyr the most stable. Although minor differences are observed in the rate constants for the reactions initiated by the two oxidants used in these studies, the results obtained for each lie in the same range. In the presence of hexachloroiridate a "lag phase" is seen at the beginning of the autoreduction process, which is not obvious in the case of ferricyanide oxidation. The origin of this "lag phase" is not yet clearly defined but most likely reflects oxidation, by the more powerful $IrCl_6^-$ oxidant, of reducing equivalents that are released during the initial stages of cluster degradation.

*NMR Characterization of Mutants.* Resonances from hyperfine-shifted protons in the reduced and oxidized mutants show some variation relative to the native spectrum, although shifts in resonance positions were typically <1 ppm. The most prominent change observed in these spectra includes the upfield shift of the $\beta$-CH resonance for Cys77 in the Phe66Tyr mutant from 12.73 to 10.95 ppm. Relative to the magnitude of the chemical shift changes for other resonances, this shift indicates a specific perturbation to Cys77, either in the form of a minor change of dihedral angle of the H−C−S−Fe bond, as recently defined by Bertini et al. (1995a) and/or by formation of a hydrogen bond from the Tyr hydroxyl to the sulfur center. A structural analysis by computer graphics indicates that the latter is a reasonable possibility, although it is difficult to distinguish between these two options. Perturbation of the remaining hyperfine-shifted signals suggests that most of these shifts arise from minor perturbations to the H−C−S−Fe dihedral angles (Bertini et al., 1995a). There appears to be a minimal perturbation of the electronic structure of the cluster, and changes in the spectrum arise from local steric effects and polarity changes that are specific for individual Cys protons. The temperature dependence of the shifted signals was examined from 5 to 35 °C and was found in all cases to be similar to that previously reported for native HiPIP with each resonance showing anti-Curie behavior (Bertini et al., 1992; Banci et al., 1993).

Over a period of 1−2 h, the spectra of oxidized mutant HiPIPs (Phe66Cys, Phe66Ser, Phe66Asn) were observed to change to the reduced form. No other hyperfine-shifted signals were observed, although new signals were observed in the diamagnetic region that are reminiscent of apo-HiPIP. Integration of the shifted resonances indicated that a substantial fraction of the holoprotein (≥ 20%) had degraded. The extent of degradation depended on both the delay time and the amount of oxidant added. More extensive degradation was observed after longer times and in the presence of larger amounts of oxidant.

Cross-peak patterns for the NH−$C^{\alpha}$H fingerprint and aromatic regions of standard 2D COSY maps taken in the diamagnetic region for Phe66 mutants were similar to those for native HiPIP. Minor changes in chemical shift were evident for some resonances in the fingerprint region, although the aromatic region shows a very similar pattern of cross-peaks. Spectral perturbations were more prominent for the Phe66Ser and Phe66Asn mutants. This affords some insight on the origin of the instability of the oxidized cluster inasmuch as the structural perturbations appear to follow the order Phe66Asn > Phe66Ser > Phe66Cys > Phe66Tyr ~ rec-native, which is consistent with the kinetic data on the stability of the oxidized mutants.

Figure 3 shows a collection of $^1H-^{15}N$ HMQC spectra obtained over a series of time intervals for each mutant and native HiPIP. The time (in minutes) marked on each spectrum corresponds to the midpoint time for the acquisition of that spectrum (each spectrum takes ~10 min to acquire) after the $^2H/^1H$ exchange was initiated. Cross-peak assignments have previously been made for native HiPIP (Li et al., 1995; Banci et al., 1995). While there is some ambiguity for assignment of the mutant proteins by inspection, a simple qualitative comparison yields significant insight on structural variations over this series of protein derivatives.

Both the native and Phe66Tyr proteins show significantly slower exchange of backbone amide protons relative to the Phe66Ser, Phe66Cys, and Phe66Asn mutants. Approximately 15 min after the exchange reaction has begun, more than half of the total NH protons still show in the native and Phe66Tyr spectra, while less than a quarter of the cross-peak signals appear in the other three mutants. The cross-peaks observed in the 15 min spectra of the Phe66Ser, Phe66Cys, and Phe66Asn mutants are mostly those that remain in the 172 min spectra of the native and Phe66Tyr proteins. It is clear, therefore, that mutation of Phe66 to Ser, Cys, or Asn leads to an increase in solvent accessibility of the protein, especially for residues in the neighborhood of the amino terminus.

Three tryptophan residues are located in the aromatic pocket for the iron−sulfur cluster. It is noted for the Phe66Ser, Phe66Asn, and Phe66Cys mutants that one of the $N^{\epsilon}H$ signals lying at about (10, 129) ppm for either Trp60 or Trp76 (Morgan et al., 1984) and the $N^{\epsilon}H$ signal of Trp80 at (10.6, 132) ppm in the Phe66Cys mutant do not show up even in the 15 min spectra, indicating that these protons are in fast exchange.

*EPR of Mutant and Deuterium-Labeled Proteins.* In common with the native protein, reduced Phe66 HiPIP mutants are EPR inactive. However, immediately after oxidation, these derivatives display EPR features (Figure 4) that are similar to the native protein, with a major axial component ($g_{||} \sim 2.03$, $g_{\perp} \sim 2.12$) and evidence of a minor component with $g \sim 2.07$ that has previously been ascribed to HiPIP solution species that differ in either their aggregation state or electronic configuration (Bertini et al., 1992; Banci et al., 1993; Antanaitas & Moss, 1975; Dunham et al., 1991). When ferricyanide was used as oxidant, the Phe66Cys and Phe66Ser mutants demonstrated additional fine features near $g_{\perp} = 2.12$, which could be simulated by including an additional minor component (Table 3 and Figure 5). These features disappeared gradually after oxidation. When hexachloroiridate was used as oxidant, the line width of the $g_{\perp}$ signal was found to be narrower than that obtained by

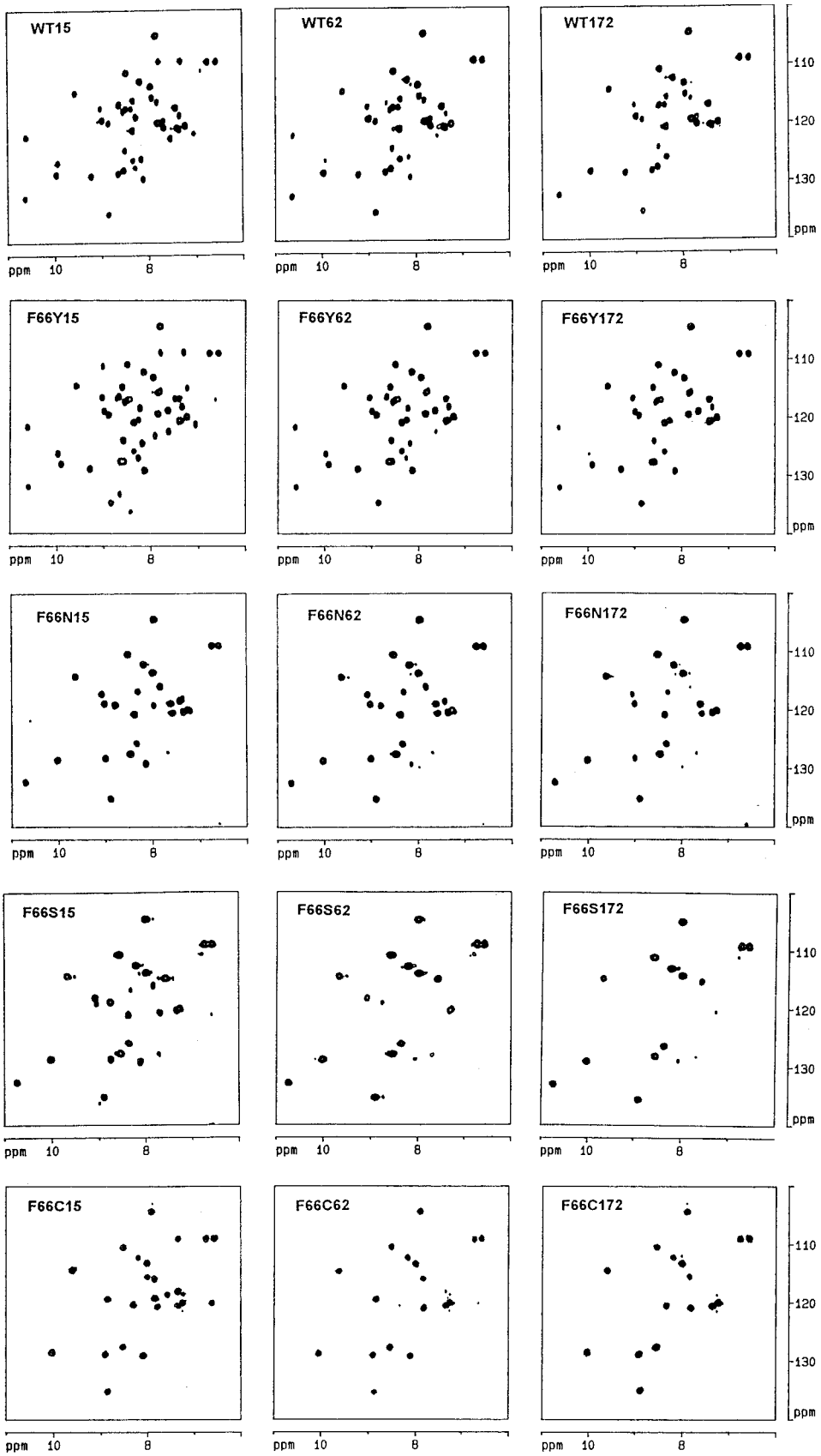


FIGURE 3: $^{1}H-^{15}N$ HMQC spectra of rec-native and mutant HiPIP's. Spectra are taken at three time intervals after the addition of $D_2O$ to a sample that has been lyophilized from a buffered $H_2O$ solution. The time lapse to the middle of the 10 min acquisition period is given immediately after the descriptor for the spectrum.

ferricyanide oxidation, while additional fine features were also observed near $g_{||} \sim 2.03$ for native protein and the Phe66Tyr mutants. For native and mutant proteins, the EPR signals were not observable at temperatures above 60 K.

With the exception of the Phe66Tyr mutant, which proved to be fairly stable, the oxidized mutant EPR signals were found to disappear when the sample was maintained at ambient temperatures after oxidation. However, a new axial

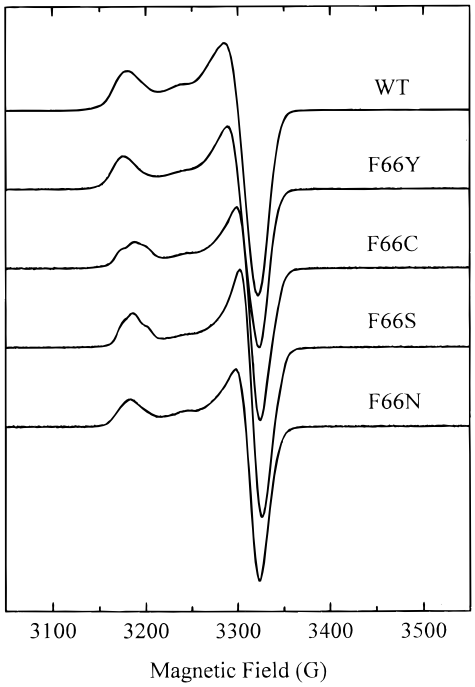


FIGURE 4: EPR spectra of oxidized rec-native and mutant HiPIP obtained with 0.7 mM protein in 20 mM potassium phosphate buffer (pH 7). The samples were frozen in liquid nitrogen immediately following oxidation with ferricyanide ion. Experimental conditions were as follows: microwave frequency 9.45 GHz; modulation frequency 100 kHz; modulation amplitude 1 G; microwave power 1.2 mW; temperature 15 K.

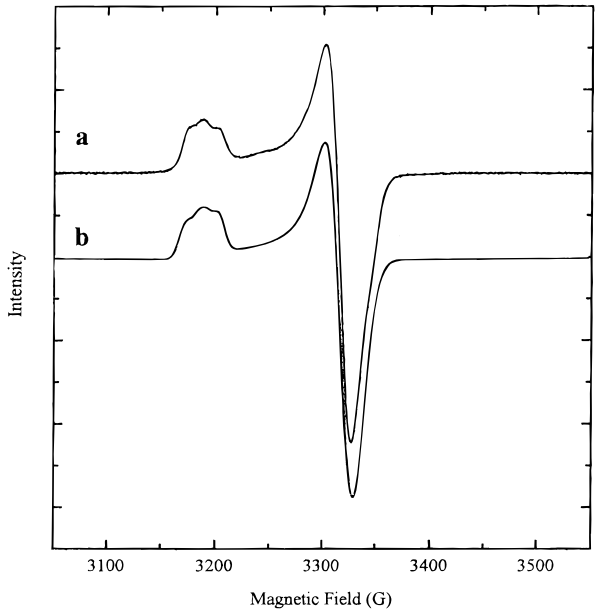


FIGURE 5: (a) EPR spectrum of Phe66Ser HiPIP obtained immediately after oxidation. The mutant protein was labeled with deuterated Cys-$d_2$, however, deuteration is not the origin of the fine splitting on the lower field signal. Sample preparation and conditions were similar to that described in the legend to Figure 4. (b) Computer simulation of the spectrum (see Table 3 for the simulation parameters). The EPR spectrum was obtained with a microwave frequency of 9.458 GHz, a modulation frequency of 100 kHz, a modulation amplitude of 4 G, a microwave power of 1.3 mW, and a temperature of 15 K.

Table 3: EPR Parameters for the Major Components of Oxidized Native and Phe66 Mutants[a]

| | rec-native | Phe66Tyr | Phe66Cys | Phe66Ser | Phe66Asn |
|---|---|---|---|---|---|
| $g_\perp$ | 2.125 | 2.126 | 2.118 | 2.119 | 2.120 |
| $A_\perp$ (G) | 15 | 14 | 15 | 14 | 14 |
| $g_\parallel$ | 2.038 | 2.038 | 2.034 | 2.033 | 2.034 |
| $A_\parallel$ (G) | 18 | 18 | 16 | 14 | 16 |

[a] Parameters were obtained by simulation as shown in Figure 5.

Table 4: EPR Parameters for the Intermediate Observed during Decay of Oxidized Phe66 Mutants[a]

| | Phe66Cys | Phe66Ser | Phe66Asn |
|---|---|---|---|
| $g_\perp$ | 2.026 | 2.028 | 2.030 |
| $A_\perp$ (G) | 10 | 11 | 11 |
| $g_\parallel$ | 2.002 | 2.006 | 2.008 |
| $A_\parallel$ (G) | 23 | 24 | 21 |

[a] Parameters were obtained by simulation as shown in Figure 6.

signal, almost isotropic with $g \sim 2.01$ ($g_\parallel = 2.00$, $g_\perp = 2.02$), was observed to grow in for the Phe66Cys, Phe66Ser, and Phe66Asn mutants (Table 4 and Figure 6). Subsequently, this signal was also observed to decay. The time frame for appearance of the signal was shorter than that for formation of the autoreduced protein for each mutant. This signal was weaker than that for the starting oxidized form and integrated to ~13% of the latter. The signal could not be detected at temperatures above 30 K. We had earlier speculated on the possibility of an internal reduction pathway to rationalize the autoreduction reaction. It seemed possible that this $g \sim 2.01$ signal might be related to such a process since it is similar to the signal obtained for a cysteinyl radical species formed in *Azotobacter vinelandii* ferredoxin oxidation, (Hu et al., 1994). If this was indeed the case, it would most likely be one of the cysteine ligands to the $Fe_4S_4$ cluster since it appears in all three of the Phe66Cys, -Ser, and -Asn mutants. However, organic radical EPR signals can be seen at higher temperatures, and in the case of the cysteinyl radical species identified in Fd I, the signal was observed at temperatures up to 77 K (Morgan et al., 1984, 1985). In contrast, the signal that is reported here, and shown in Figure 6, was not observed at temperatures greater than 30 K. Furthermore, no significant line-broadening was observed in cysteine-$d_2$-labeled mutant HiPIP's, expected of a cysteinyl radical, and so other possibilities were considered. In particular, the $g \sim 2.01$ signal is very similar to the [$Fe_3S_4$]$^+$ cluster signal observed in oxidized ferredoxin (Emptage et al., 1980; Papaefthymiou et al., 1987) and mutants of DMSO reductase (Rothery & Weiner, 1991). Figure 7 shows typical EPR power saturation plots for oxidized mutant HiPIP taken immediately after oxidation, corresponding to [$Fe_4S_4$]$^{3+}$, and 48 h after oxidation (incubating at 4 °C) to allow a buildup of the intermediate species. The signal intensity, $S$, was plotted against the power, $P$, and the data fit by use of eq 3 (Beinert & Orme-Johnson, 1967; Innes & Brudvig, 1989). The half-power saturation, $P_{1/2}$, is defined by the turning point of the curve, and power saturation parameters for the fitted data are summarized in Table 5. Optimal fits were obtained with a b value close to 1, corresponding to the inhomogeneous limit often observed for signals from Fe-S centers. A $P_{1/2}$ of 16 mW was determined for the signal observed from the immediately oxidized HiPIP, while the intermediate decay signal shows very different power saturation behavior. The lowest power used in this experiment is very close to the saturation limit of the autoreduced signal, which is below 400 $\mu$W and is again characteristic of oxidized $Fe_3S_4$ clusters (Rothery & Weiner, 1991; Rupp et al., 1978, 1979).

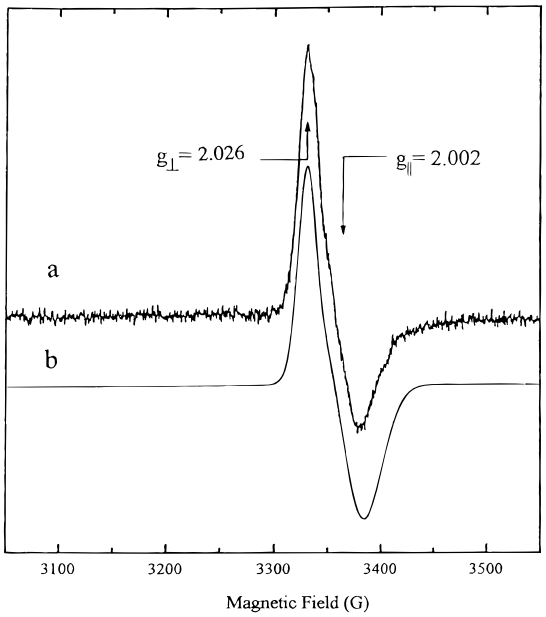


FIGURE 6: (a) EPR spectrum of the intermediate formed following oxidation of Phe66Cys HiPIP. The sample, containing 0.7 mM protein in 20 mM potassium phosphate buffer (pH 7), was allowed to remain at room temperature for several hours following oxidation with ferricyanide before freezing in liquid nitrogen. (b) Computer simulation of the spectrum (see Table 4 for the simulation parameters). The EPR spectrum was obtained with a microwave frequency of 9.456 GHz, a modulation frequency of 100 kHz, a modulation amplitude of 1 G, a microwave power of 1.2 mW, and a temperature of 15 K.

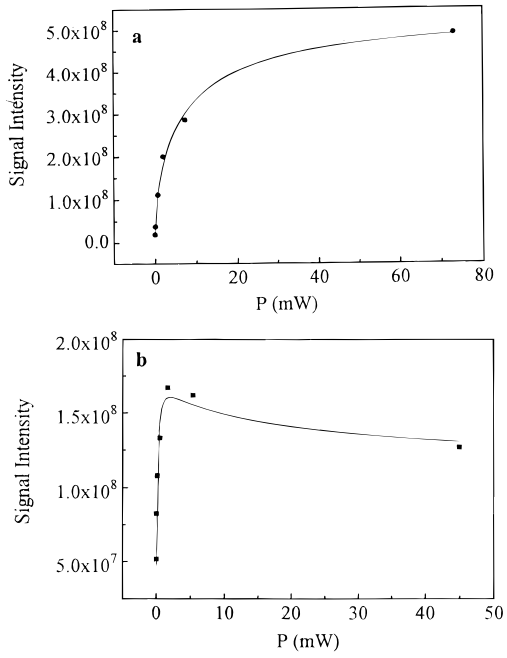


FIGURE 7: (a) EPR power saturation study on the signals from Phe66Asn HIPIP immediately after oxidation. The EPR spectrum was obtained with a microwave frequency of 9.455 GHz, a modulation frequency of 100 kHz, a modulation amplitude of 0.5 mT, a receiver gain of $10^4$, and a temperature of 15 K. (b) EPR power saturation study on the signals from Phe66Asn HIPIP after formation of the decay immediate following oxidation. The EPR spectrum was obtained with a microwave frequency of 9.457 GHz, a modulation frequency of 100 kHz, a modulation amplitude of 5 G, a receiver gain of $10^4$, and a temperature of 15 K.

In a valence-localized model we may assume loss of the ferrous ion, yielding an oxidized $[Fe_3S_4]^+$ core with $S = {}^1/_2$. This proposal explains the appearance of the $Fe_3S_4$ cluster signal but does not account for the remainder of the sample, since only ~13% of the 3Fe cluster is transiently formed on the basis of EPR integration. Also, there is no evidence for the presence of a $[Fe_3S_4]$ cluster protein intermediate in NMR spectra of the autoreduced sample, consistent with our interpretation of this center as a transient intermediate, which forms and subsequently decays. Minor peaks are observed at earlier stages of the reduction pathway; however, these are too weak to be characterized with any certainty. These observations are fully consistent with the reaction pathway summarized in Scheme 1, where degradation of the cluster in step 1 provides the reducing equivalents ($S^{2-}$ and $Fe^{2+}$ ions) that result in reduction of the remainder of the sample in step 2. The relative rates of these reaction steps remain to be defined. Cluster degradation to form apoprotein was quantitated by comparison of integrations of 1D proton NMR spectra, and by the appearance of NMR resonances from apo-HiPIP, and appears to proceed by way of the $[Fe_3S_4]^+$ center.

Table 5: EPR Power Saturation Parameters for the Major Component EPR Signals of Oxidized Phe66Asn[a]

| | initial signal | intermed signal |
|---|---|---|
| $P_{1/2}$ (mW) | 16 | 0.4 |
| $K$ ($mW^{1/2}$) | $1.36 \times 10^8$ | $3.3 \times 10^8$ |
| $b$ | 1.0 | 1.2 |

[a] Parameters were obtained by fitting to the standard equation, $S = K[P/(1 + P/P_{1/2})^b]^{1/2}$.

Scheme 1

$$HP_{ox}[Fe_4S_4]^{3+} \xrightarrow[-Fe^{2+}]{} HP_{ox}[Fe_3S_4]^{+} \rightarrow HP_{apo} + 3Fe^{3+} + 4S^{2-} \quad (1)$$

$$HP_{ox}[Fe_4S_4]^{3+} \xrightarrow[Fe^{2+}/S^{2-}]{} HP_{red}[Fe_4S_4]^{2+} \quad (2)$$

## DISCUSSION

*Influence of Mutations on the Electronic Properties of the Cluster.* A variety of nonconservative mutations have been made at residue Phe66 of *C. vinosum* HiPIP, a paramagnetic iron−sulfur protein. These mutations show only a small influence on the cluster reduction potential and result in a general increase in $E_m$. The largest change was observed following replacement of Phe with the amide side chain of Asn (Soriano et al., 1996). Significant perturbations were also observed for the shifted resonances in the $^1H$ NMR spectrum of this mutant, although these changes were specific to the Cys63 residue coordinated to the cluster and did not indicate a general perturbation of the electronic structure of the cluster. It is likely that the larger than usual (~40 mV) increase in $E_m$ for Phe66Asn reflects either minor structural changes in the active site and/or the influence of the amide dipole. Although the Phe66Asn mutant shows the most significant increase in solvent accessibility, this is unlikely to underlie the observed change in $E_m$ since the change in solvation for Phe66 mutants is less than we have previously observed for Tyr19 mutants, many of which showed smaller changes in $E_m$. These results support a general conclusion from recent work in our laboratory (Agarwal et al., 1995, 1996), and other groups (Shen et al., 1993, 1994; Babini et

al., 1996), that the side chains forming the cluster pocketserve little role in the definition of gross reduction potential. Our results do, however, indicate a general and important role in maintaining cluster stability.

In view of these results, it is likely that the shift of $\sim -50$ mV in the opposite direction observed for the *R. tenuis* HiPIP relative to the *C. vinosum* protein does not arise from the replacement of a Phe with Ile in the former, with the consequent change in local polarity in the cluster pocket or loss of binding interactions between the aromatic side chain and the cluster. Since there is unlikely to be a significant change in solvent accessibility (the oxidized cluster in *R. tenuis* HiPIP is stable), the difference in $E_m$ most likely reflects a global perturbation of the net dipole from the backbone amides (Jensen et al., 1994).

*Cluster Stability*. Nonconservative mutations of residue Phe66 have been found to introduce significant instability to the prosthetic $Fe_4S_4$ cluster. This instability appears to stem from the increase in solvent accessibility to the cluster core. This is made evident by comparison of the fingerprint region of 2D COSY spectra and $^1H-^{15}N$ HMQC spectra (Figure 3) where a significant number of cross-peaks are absent relative to the native protein. Other prominent losses include the cross-peaks from ring NH protons located on Trp residues in the cluster cavity. The extent of solvent accessibility was found to be significantly lower than that exhibited by Tyr19 mutants. The latter have been extensively described in recent reports from our laboratory (Agarwal et al., 1995; Li et al., 1996b). In brief, Tyr19 is located at an entrance cleft to the hydrophobic pocket and serves to maintain a hydrophobic barrier for exclusion of water from the cluster cavity. Tyr19 mutant proteins demonstrate, to varying extents, the ability of water molecules to exchange with ionizable protons in the cluster binding pocket, and solvent accessibility resulted in facile oxidation of the cluster by atmospheric oxygen, with subsequent rapid hydrolysis of the $[Fe_4S_4]^{3+}$ core. Such a decrease in cluster stability in the presence of a polar solvent is consistent with previous studies of model complexes that demonstrate sensitivity of the oxidized $[Fe_4S_4]^{3+}$ core to solvolytic decomposition (O'Sullivan & Millar, 1985; Maskiewicz & Bruice, 1977; Roth & Jordanov, 1992; Blonk et al., 1991; Nakamoto et al., 1988).

We have observed that solvent accessibility to the cluster pocket is diminished for Phe66 mutants relative to those for Tyr19, and so degradation of the cluster occurs at a slower rate. The consequences of reduced solvent accessibility for the Phe66 mutants are 2-fold. First, reducing equivalents provided by the disintegrating cluster (one ferrous ion and four sulfides) may serve to reduce the remainder of the oxidized protein. This results in an apparent autoreduction pathway. Such a pathway is supported by comparison of the relative integrations from 1D NMR spectra obtained for reduced mutant proteins before oxidation and following autoreduction. Integration of the paramagnetically shifted resonances shows that $\geq 20\%$ of the starting protein is lost, presumably reverting to apoprotein as evidenced by changes in the diamagnetic region indicative of apo-HiPIP. As expected, the extent of degradation increases with the concentration of oxidant, which can either reoxidize the autoreduced protein or consume the reducing equivalents made available by cluster degradation. There are no additional hyperfine-shifted peaks in the spectrum of the final autoreduced sample that would indicate a stable iron-containing species. Such an autoreduction pathway has precedent in small molecule analog chemistry.

The second consequence of the more tardy decomposition rate is the appearance of an apparent intermediate in the decomposition pathway. This is cleanly detected by low-temperature EPR spectroscopy after the sample is held at ambient temperature for $\sim$20 min to 1 h, depending on the mutant and the ambient temperature (varying from 4 to 25 °C). Relative to the oxidized protein, this species represents $\sim$13% of the starting sample, as determined by integration of the EPR signals. Over time this signal also diminishes, consistent with its assignment as a degradation intermediate, although the microscopic rate constants for formation and degradation of this intermediate have not yet been amenable to evaluation. Amino acid radical centers were considered; however, with the exception of cysteine radical, the observed EPR features are unlike those observed for other residue-centered radicals, including Gly, Phe, and Tyr. The possibility of a cysteine radical was excluded by labeling with Cys-$d_2$: no splitting or broadening was observed in the EPR bands. As an alternative we considered the possibility of an $[Fe_3S_4]^+$ center. The appearance of the spectrum, and the temperature and power dependence of the spectral features are consistent with previous observations on such metallocluster centers. There is also extensive evidence from model studies for oxidative conversion of a $[Fe_4S_4]^{3+}$ core to a $[Fe_3S_4]^+$ center and subsequent degradation in nucleophilic solvents (Roth & Jordanov, 1992). In enzyme systems, oxidative conversion to a $[Fe_3S_4]^+$ center was first reported for mammalian aconitase (Kennedy et al., 1983) and proposed for succinate-ubiquinone reductase (complex II) (Ackrell et al., 1984), although in the latter case the 3Fe center is now known to be the naturally occurring form of the cluster in the succinate-fumarate oxidoreductase enzymes (reviewed in Matsubara & Saeki, 1992).

These data again demonstrate a quite distinct role from that previously postulated for the aromatic core residues of high-potential iron proteins. In the oxidized state the cluster is sensitive toward hydrolytic decomposition. The hydrophobic aromatic core residues apparently maintain a barrier toward exclusion of solvent. This idea was developed by Stout in earlier comparisons of the $[Fe_4S_4]$ cluster environment in high- and low-potential ferredoxins (Stout, 1982). Our results for both Tyr19 and Phe66 mutants indicate that such residues have little role in defining the reduction potential of the cluster. Relative to the influence of Tyr19 mutants the increase in solvent accessibility is less pronounced for the Phe66 derivatives and is consistent with the positions of each residue. Tyr19 forms a barrier between the cluster pocket and bulk solvent, while Phe66 lies within the cluster and mediates its effect less directly. Two possible mechanisms for solvent access in the Phe66 mutants include the introduction of a general conformational flexibility that facilitates solvent exchange or the leakage of solvent at a specific location. Finally, it may be noted that core aromatic residues have been frequently cited as important mediators of electron-transfer reactions. Such a role is distinct from the model described above and is not supported by measurements of electron self-exchange rates for Phe66, Phe48, and Tyr19 mutants (Soriano et al., 1996).

## REFERENCES


Aasa, R., & Vanngard, T. (1975) *J. Magn. Reson. 19*, 308.

Ackrell, B. A. C., Kearney, E. B., Mims, W. B., Peisach, J., & Beinert, H. (1984) *J. Biol. Chem. 259*, 4015.

Agarwal, A., Tan, J., Eren, M., Tevelev, A., Lui, S. M., & Cowan, J. A. (1993) *Biochem. Biophys. Res. Commun. 197*, 1357−1362.

Agarwal, A., Li, D., & Cowan, J. A. (1995) *Proc. Natl. Acad. Sci. U.S.A. 92*, 9440−9444.

Agarwal, A., Li, D., & Cowan, J. A. (1996) *J. Am. Chem. Soc. 118*, 927−928.

Antanaitis, A., & Moss, T. H. (1975) *Biochim. Biophys. Acta 465*, 262.

Babini, E., Bertini, I., Borsari, M., Capozzi, F., Dikiy, A., Eltis, L. D., & Luchinat, C. (1996) *J. Am. Chem. Soc. 118*, 75.

Banci, L., Bertini, I., Ciurli, S., Ferretti, S., Luchinat, C., & Picioli, M. (1993) *Biochemistry 32*, 9387.

Banci, L., Bertini, I., Dikiy, A., Kastrau, D. H. W., Luchinat, C., & Sompornpisut, P. (1995) *Biochemistry 34*, 206.

Bartsch, R. G. (1978) *Methods Enzymol. 53*, 329−340.

Beinert, H., & Orme-Johnson, W. H. (1967) *Magn. Reson. Biol. Syst.* 221−247.

Bell, S. H., Dickson, D. P., Johnson, C. E., Cammack, R., Hall, D. O., & Rao, K. K. (1982) *FEBS Lett. 142*, 143.

Bertini, I., Ciurli, S., Dikiy, A., & Luchinat, C. (1992) *J. Am. Chem. Soc. 114*, 12020.

Bertini, I., Gaudemer, A., Luchinat, C., & Piccioli, M. (1993) *Biochemistry 32*,, 12887.

Bertini, I., Capozzi, F., Eltis, L. D., Felli, I. C., Luchinat, C., & Piccioli, M. (1995a) *Inorg. Chem. 34*, 2516−2523.

Bertini, I., Dikiy, A., Kastrau, D. H. W., Luchinat, C., & Sompornpisut P. (1995b) *Biochemistry 34*, 9851.

Blonk, H. L., Kievit, O., Roth, E. K. H., Jordanov, J., van der Linden, J. G. M., & Steggerda, J. J. (1991) *Inorg. Chem. 30*, 3231−3234.

Carter, C. W., Jr. (1977) in *Iron-sulfur Proteins III* (Lovenberg, W., Ed.) pp 157−204, Academic Press, New York.

Carter, C. W., Jr., Kraut, J., Freer, S. T., Xuong, N. H., Alden, R. A., & Bartsch, R. G. (1974a) *J. Biol. Chem. 249*, 4212.

Carter, C. W., Kraut, J., Freer, S. T., Xuong, N. H., & Alden, R. A. (1974b) *J. Biol. Chem. 249*, 6339.

Dunham, W. R., Hagen, W. R., Fee, J. A., Sands, R. H., Dunbar, J. B., & Humblet, C. (1991) *Biochim. Biophys. Acta 1079*, 253.

Emptage, M. H., Kent, T. A., Huynh, B. H., Rawlings, J., Orme-Johnson, W. H., & Munck, E. (1980) *J. Biol. Chem. 255*, 1793.

Fee, J. A. (1975) *Methods Enzymol. 49*, 512−528.

Flint, D. H. (1996) *J. Biol. Chem. 271*, 16068−16074.

Flint, D. H., Tuminello, J. F., & Emptage, M. H. (1993) *J. Biol. Chem. 268*, 22369−22376.

Flint, D. H., Tuminello, J. F., & Miller, T. J. (1996) *J. Biol. Chem. 271*, 16053−16067.

Hu, Z., Jollie, D., Burgess, B. K., Stephens, P. J., & Munck, E. (1994) *Biochemistry 33*, 14475−14485.

Innes, J. B., & Brudvig, G. W. (1989) *Biochemistry 28*, 1116.

Inubushi, T., & Becker, E. D. (1983) *J. Magn. Reson. 51*, 128.

Jensen, G. M., Warshel, A. J., & Stephens, P. J. (1994) *Biochemistry 33*, 10911.

Johnson, M. K., Spiro, T. G., & Mortenson, L. E. (1982) *J. Biol. Chem. 257*, 2447.

Kay, E., Keifer, P., & Saarinen, T. (1992) *J. Am. Chem. Soc. 114*, 10663.

Kennedy, M. C., Emptage, M. H., Dreyer, J. L., & Beinert, H. (1983) *J. Biol. Chem. 258*, 11098.

Kowal, A. T., Werth, M. T., Manodori, A., Cecchini, G., Schroeder, I., Gunsalus, R. P., & Johnson, M. K. (1995) *Biochemistry 34*, 12284−12293.

Kunkel, T. A., Roberts, J. D., & Zakour, R. A. (1987) *Methods Enzymol. 154*, 267−382.

Li, D., Cottrell, C. E., & Cowan, J. A. (1995) *J. Protein Chem. 4*, 115.

Li, D., Soriano, A., & Cowan, J. A. (1996a) *Inorg. Chem. 35*, 1980−1987.

Li, D., Agarwal, A., & Cowan, J. A. (1996b) *Inorg. Chem. 35*, 1121−1125.

Lui, S. M., & Cowan, J. A. (1994) *J. Am. Chem. Soc. 116*, 4483.

Maskiewicz, R., & Bruice, T. C. (1977) *Proc. Natl. Acad.Sci. U.S.A. 74*, 5231.

Matsubara, H., & Saeki, K. (1992) *Adv. Inorg. Chem. 38*, 223 −280.

Mizrahi, I. A., Meyer, T. E., & Cusanovich, M. A. (1980) *Biochemistry 19*, 4727.

Morgan, T. V., Stephens, P. J., Devlin, F., Stout, C. D., Melis, K. A., & Burgess, B. K. (1984) *Proc. Natl. Acad. Sci. U.S.A. 81*, 1931.

Morgan, T. V., Stephens, P. J., Devlin, F., Burgess, B. K., & Stout, C. D. (1985) *FEBS Lett*. 206.

Moura, J. J. G., Moura, I., Kent, T. A., Lipscomb, J. D., Huynh, B. H. LeGall, J., Xavier, A. V., & Munck, E. (1982) *J. Biol. Chem. 257*, 6259.

Nakamoto, M., Tanaka, K., & Tanaka, T. (1988) *J. Chem. Soc., Chem. Commun.* 1422.

O'Sullivan, T., & Millar, M. M. (1985) *J. Am. Chem. Soc. 107*, 44096.

Pagani, S., Bonomi, F., & Cerletti, P. (1984) *Eur. J. Biochem. 142*, 361.

Palmer, A. G., Cavanagh, J., Wright, P. E., & Rance, M. (1991) *J. Magn. Reson. 93*, 151.

Papaefthymiou, V., Girerd, J.-J., Moura, I., Moura, J. G., & Munck, E. (1987) *J. Am. Chem. Soc. 109*, 4703.

Przysieck, C. T., Meyer, T. E., & Cusanovich, M. A. (1985) *Biochemistry 24*, 2524.

Rayment, I., Wesenberg, W., Meyer, T. E., Cusanovich, M. A., & Holden, H. M. (1992) *J. Mol. Biol. 228*, 672−686.

Roth, E. K. H., & Jordanov, J. (1992) *Inorg. Chem. 31*, 324−243.

Rothery, R. A., & Weiner, J. H. (1991) *Biochemistry 30*, 8296.

Rupp, H., Rao, K. K., Hall, D. O., & Cammack, R. (1978) *Biochem. Biophys. Acta 537*, 255−269.

Rupp, H., de la Torre, A., & Hall, D. O. (1979) *Biochem. Biophys. Acta 548*, 552−564.

Sambrook, J., Fritsch, E. F., & Maniatis, T. (1989) *Molecular Cloning*, Vols. I−III, Cold Spring Harbor Laboratory Press, Cold Spring Harbor, NY.

Schleucher, J., Sattler, M., & Griesinger, C. (1993) *Angew. Chem. Int. Ed. Engl. 32*, 1489−1491.

Shen, B., Martin, L. L., Butt, J. N., Armstrong, F. A., Stout, C. D., Jensen, G. M., Stephens, P. J., La Mar, G. N., Gorst, C. M., & Burgess, B. K. (1993) *J. Biol. Chem. 268*, 25928.

Shen, B., Jollie, D. R., Stout, C. D., Diller, T. C., Armstrong, F. A., Gorst, C. M., La Mar, G. N., Stephens, P. J., & Burgess, B. K. (1994) *J. Biol. Chem. 269*, 8564.

Soriano, A., Li, D., Bian, S., Agarwal, A., & Cowan, J. A. (1996) *Biochemistry 35*, 12479−12486.

Stout, C. D. (1982) in *Metal Ions in Biology* (Spiro, T. G., Ed.) Vol. 4, Chapter 3, John Wiley and Sons, New York.

Thomson, A. J., Robinson, A. E, Johnson, M. K., Cammack, R., Rao, K. K., & Hall, D. O. (1981) *Biochim. Biophys. Acta 637*, 423.


BI961658L